sciendo

POLISH MARITIME RESEARCH 4 (112) 2021 Vol. 28; pp. 42-52
10.2478/pomr-2021-0048

THE INFLUENCE OF SELECTED STRAIN-BASED FAILURE CRITERIA ON SHIP STRUCTURE DAMAGE RESULTING FROM A COLLISION WITH AN OFFSHORE WIND TURBINE MONOPILE

Karol Niklas*
Alicja Bera
Gdańsk University of Technology, Poland

* Corresponding author: *karol.niklas@pg.edu.pl (K. Niklas)*

ABSTRACT

Offshore wind farms are developing well all over the world, providing green energy from renewable sources. The evaluation of possible consequences of a collision involves Finite Element computer simulations. The goal of this paper was to analyse the influence of selected strain-based failure criteria on ship damage resulting from a collision with an offshore wind turbine monopile. The case of a collision between an offshore supply vessel and a monopile-type support structure was examined. The results imply that simulation assumptions, especially the failure criteria, are very important. It was found that, using the strain failure criteria according to the minimum values required by the design rules, can lead to an underestimation of the ship damage by as much as 6 times, for the length of the hull plate, and 9 times, for the area of the ship hull opening. Instead, the adjusted formula should be used, taking into account both the FE element size and the shell thickness. The influence of the non-linear representation of the stress-strain curve was also pointed out. Moreover, a significant influence of the selected steel grade on collision damages was found.

Keywords: Ship, collision, monopile, failure, crashworthiness

INTRODUCTION

The offshore production of energy from wind is developing dynamically (see Fig. 1 and Fig. 2). Large wind farm projects are underway on the Baltic Sea. Offshore wind farms are often located in the immediate vicinity of busy shipping routes and near coastlines with restricted areas. Key trends and statistics indicate dynamic development of the offshore wind energy sector [1-2]. This increases the risk of collisions between ships and wind farm support structures, which can lead to major damage to the environment and enormous financial losses. About 3,300 ships are involved in accidents each year. Collisions and groundings account for 43% of all accidents [3].

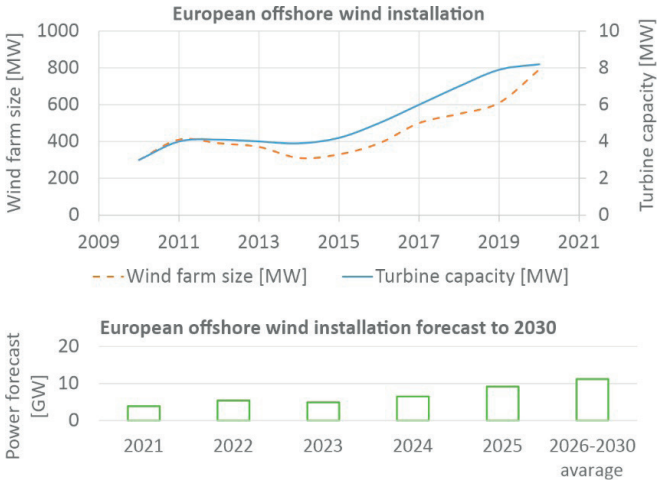

Fig. 1. European offshore wind farm installations (2010-2020) and the forecast until 2030 [2]

Fig. 2. Sample photograph of an offshore support vessel (OSV) operating at an offshore wind turbine (OWT) farm [1]

These issues are important and have been the subject of numerous scientific studies. Safety at sea is very important, therefore research has been carried out on various ocean engineering structures for different purposes and dynamics [4-12]. For example, an analysis of ship collisions with 3 types of support structures was published by [13]. The effects of the collisions on the support structures were analysed and the jacket was found to be the most robust structure type. The paper pointed out the strong influence of Finite Element (FE) computer simulation assumptions on the results. On the other hand, paper [14] presented the strength analysis of a large gravity type foundation, [15] presented strength analysis of a Tripile-type support structure and [16] showed the problems associated with the long-term use of structures at sea. However, by far the most common type of support structures used is the monopile (81% in Europe [17]), which is the subject of publications such as [18]. There are also hybrid solutions combining energy from floating wind towers and energy from sea waves [19-20]. Also, [21] and [22] studied the effect of different collision scenarios and model assumptions on the prediction of consequences of a collision between a ship and a support structure. Again, the tremendous influence of model assumptions on the results was highlighted.

Paper [23] dealt with the impact of collisions on potential damage to the turbine support column and blades. The most thorough analyses of the effect of model assumptions on collision outcome predictions to date was published in papers dealing with ship collisions and groundings, i.e. [24-28]. A benchmark study [26] of the impact of various modelling aspects has shown that the model of the material in question and the failure criteria are the two key assumptions in the computer simulation of collisions. The most commonly used are strain-based criteria, in which the range between the proposed values of failure strain for the normal-strength hull steel ranges from 0.1 to 0.7 [26], [29]. Such a wide range of values of the failure strain adopted by various authors may raise serious doubts about the reliability of the obtained results. A value of 0.2 is quite often used in ship collision simulations [26], [30] and is often assumed to be equal to the minimum material requirements specified by the design rules [31]. At the same time, the value is much smaller than that obtained from experimental material tests in the case that, as the author explained, did not take into account the geometric stress concentrations present in the finite element mesh of relatively large size. The study by [32] used a failure strain value of 0.2 in ship collision simulations. In contrast, another author recommended a rupture strain value of 0.35 while performing a series of experimental validation studies [33]. In another study [34], the Yagi at all also refers to a failure rupture value of 0.2 without providing a reference. Yet another paper [35] pointed out the huge influence of the finite element size and the plate thickness by introducing a correction equation. For the formula, much higher values of failure strain, equal to 0.39 and 0.66 (depending on the size of the element), correctly reflected the conditions of the performed experiments – pressing the sphere model into a flat plate.

A comparison of collision simulation results for different failure criteria was published in [36]. Significant discrepancies were found in the results. The need to perform a mesh convergence study was indicated, since the size of the element used has a strong effect on the simulation results. At the same time, it was pointed out that the failure criteria took into account the mesh size and the shell thickness, predicted the collision damage with the highest accuracy.

A literature study indicated that various modelling assumptions are being used, which have a significant influence on the consequences of collisions between ships and offshore support structures. Different values of the most often used strain-based failure criteria are of great importance. Therefore, this paper analyses the influence of the selected strain-based failure criteria on the ship damage caused by a collision with a monopile support structure of an offshore wind turbine (OWT). The details of the material models and the damage criteria are described in Section 3.

GOAL AND SCOPE

The goal of this paper is to investigate the influence of the selected strain-based material failure criteria on the ship damage resulting from a collision with an offshore wind turbine monopile.

The scope of the work considers two selected failure criteria. The first criterion is the constant-value strain failure (referred to in the NORSOK standard [37] and recommended by DNV GL [38]) which is taken as the minimum required strain for the material. The second failure criterion analysed is the one proposed by [24], together with the uniform strain coefficient ε_g and the necking strain coefficient ε_e proposed by [39]. Both criteria were used in numerous research projects. For both criteria, two materials were investigated: normal steel grade S235 and high-strength steel grade S355. Both materials are commonly used in the shipbuilding industry. Moreover,

the article investigates the influence of the numerical representation of a stress-strain curve of ship damage.

Two cases were analysed. The first definition of the material curve was applied according to the DNV GL 2013 design rules [40], using the simplification by characteristic points. This approach has been used for over 30 years. The second definition of the material curve was applied according to the DNV GL 2019 design rules [31]. The new version uses a more detailed representation of the non-linear range of the stress-strain curve defined by Eq. (1). The presented study also aims to assess the potential influence of the material curve representation on the collision results. So far, there have been no guidelines on this. The research was performed by FEM non-linear collision simulations using LS-dyna v. 9.71 software. The critical case of the head-on collision was investigated for three initial ship velocities: v = 2 m/s, v = 3 m/s and v = 4 m/s. The vessel was represented by a deformable structure that impacted a rigid monopile-type support structure of an offshore wind turbine. The detailed numerical model and the simulation approach are described in the following section.

THE NUMERICAL MODEL USED FOR COLLISION SIMULATIONS

The computer simulations of collisions were made in accordance with the methodology defined by the NORSOK standard [37]. The ship's structure was modelled as deformable, while the tower was assumed to be rigid. Following the NORSOK standard, the collision simulation was performed as a 'strength design' with the ship intentionally forced to deform and dissipate the collision energy (Fig. 3).

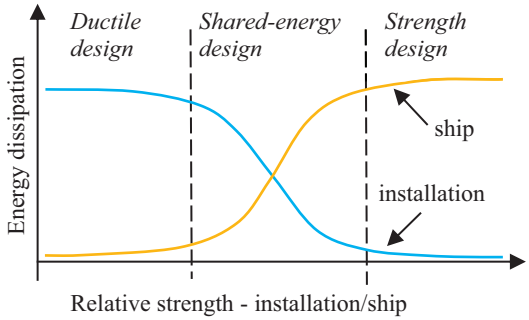

Fig. 3. Energy dissipation for strength, ductile and shared-energy design [37]

GEOMETRY, LOADS AND BOUNDARY CONDITIONS

The model of the ship and wind tower used in this study represented selected up-to-date industry-leading solutions. The geometry of the ship bow had a conical shaped hull with a bulbous bow, similar to that developed by the Havyard Company and often used in the Offshore Support Vessel (OSV). The ship length was LOA= 83.5 m, the beam was 17.5 m and the displacement was 6500 tons. The typical novel ship structure was modelled to provide adequate representation. The thickness of the hull plating varied along the height of the vessel. It was 13 mm in the bottom section, 10 mm in the transition part and 8 mm in the upper section of the vessel. The FE model of the ship was built with the use of 2 types of elements: shells (plating, bulkheads, decks, framing) and beams (stiffeners flanges). The monopile tower represented a typical support structure of a 3 MW offshore wind turbine. It was a tube with a diameter of 4.3 m. The tower height was 115 m. The FE model of the tower was built with the use of shell elements.

The monopile was modelled as a non-deformable (rigid) part. The FE model of the ship and the monopile of the OWT is shown in Fig. 4 and Fig. 5. It also shows the mutual positions of the vessel and the column at the moment of impact. The impact point was at the D-Deck (see Fig. 4 and Fig. 5) and it was similar for all the analysed cases. The head-on collision scenario was analysed with the initial ship velocity in the x-axis direction. The ship having the displacement of 6500 tons struck the tower freely. The weight of the ship's structural components, not represented in the model directly, together with the added mass representing the surrounding water was assigned to the mass element at the point of the ship's centre of gravity (COG). This element was connected to the bow structure by massless rigid beam elements. The added mass was equal to 325 tons, referring to a 0.05 mass coefficient [41]. The value of friction coefficient of 0.2 was used, as in reference [42]. The OWT structure was clamped at the base.

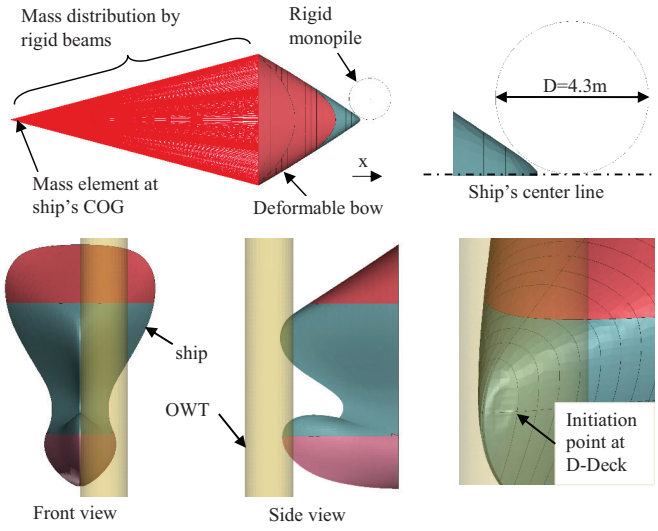

Fig. 4. The relative initial positions of the ship and the OWT monopile in the head-on collision simulation.

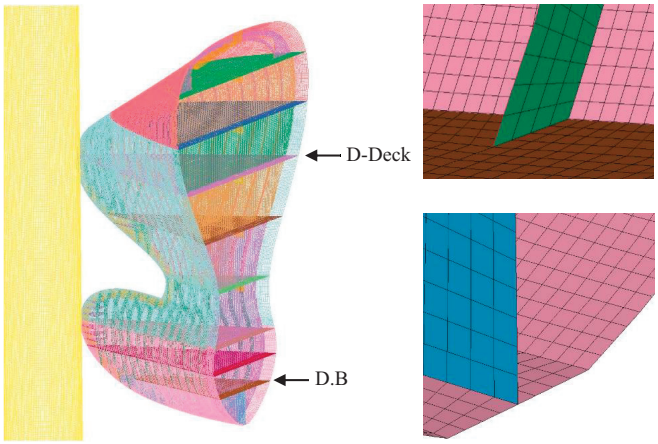

Fig. 5. The FE model of the ship's bow and the monopile (left); sample mesh details (right)

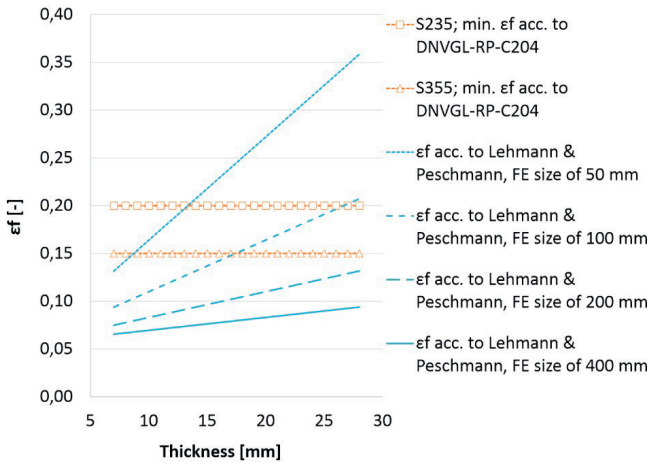

Fig. 6. Stress-strain curves representations – simplified acc. to DNVGL 2013 [40] and acc. to equation 1 and DNVGL 2019 [31].

THE MATERIAL MODEL

Two grades of steel were considered for the collision simulations: normal-strength steel S235 and high-strength steel S355. The two materials were used to analyse the influence of the selected failure criterion on the collision damage, which will be described in the next paragraph. However, it is worth noting the definitions of the stress-strain curves given by DNV GL 2013 [40] and DNV GL 2019 [31]. The latter of the recommended practices defined the non-linear stress-strain relation using Eq. (1). In contrast, the previous definition was simplified by characteristic points and straight lines. It has been used in scientific research and industrial applications for a long time. In this paper, both of these definitions were investigated to identify the influence of the material stress-strain curve simplification on the results. The material data for both steel grades is summarised in Table 1 and plotted in Fig. 6. A steel density of 7850 kg/m^3, a Young's modulus of 210 GPa and a Poisson's ratio of 0.3 were assumed. The deformable ship structure was modelled by material model *024-PIECEWISE_LINEAR_PLASTIC. The OWT monopile structure was modelled by the *020-RIGID material model.

$$\sigma = K\left(\varepsilon_p + \left(\frac{\sigma_{yeld2}}{K}\right)^{\frac{1}{n}} - \varepsilon_{p\_y2}\right)^n \quad for\ \varepsilon_p > \varepsilon_{p\_y2} \qquad (1)$$

where:
σ – stress
K, n – Ramberg-Osgood parameters
ε_p, σ_{yeld2}, ε_{py2}, ε_p – stress-strain curve parameters

The selected two strain-based failure criteria were considered in the analyses. The first criterion was according to the minimum required rupture strain value defined by the DNV GL design rules [38] and by the NORSOK standards [37]. The DNV GL rules require the minimum value of strain failure to be: 20% for the S235 and 15% for the S355 high tensile steel grades. These values were applied as modelling assumptions in many research publications [43-45].

The second criterion used in the research was introduced by [24] and is expressed as Eq. (2). This criterion includes the shell thickness, FE size, uniform strain coefficient $\varepsilon_g = 0.056$ and necking strain coefficient $\varepsilon_e = 0.54$, specified by Germanischer Lloyd [39].

$$\varepsilon_f(l_e) = \varepsilon_g + \varepsilon_e\left(\frac{t}{l_e}\right) \qquad (2)$$

where:
ε_f – failure strain,
ε_g – uniform strain,
ε_e – necking strain,
t – plate thickness,
l_e – length of a single element.

Fig. 7 shows the dependence of failure strain εf on the FE mesh size and on the shell element thickness. For the adopted element size of 100 mm and for the plate thickness ranging from 7 to 15 mm, the calculated failure strain is in a range between $\varepsilon_f = 0.0938$ and $\varepsilon_f = 0.1370$. The failure strain, ε_f, according to the analysed criteria, is shown in Fig. 8.

Tab. 1 Material properties applied in collision simulations

Material	Minimum Yield point σ_y [MPa]	Minimum Ultimate Strength σ_{ult} [MPa]	K [MPa]	n [-]	Nonlinear range of stress-strain curve	Reference
S235	235	360			Simplified by characteristic points	DNVGL 2013 [40]
S355	355	470			Simplified by characteristic points	DNVGL 2013 [40]
S235	235		520	0.166	Equation 1	
S355	355		740	0.166	Equation 1	DNVGL 2019 [31]

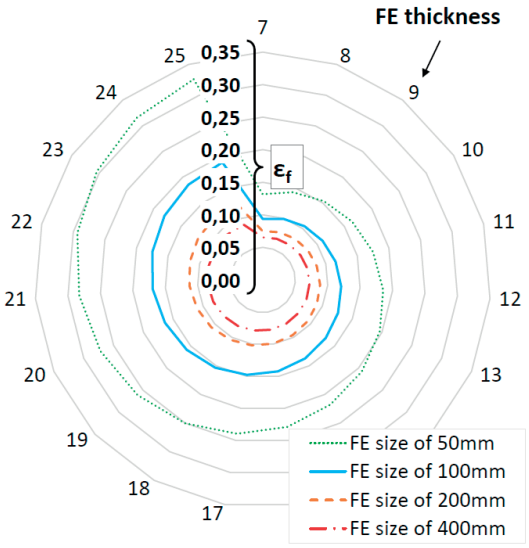

Fig. 7. Dependency of failure strain εf on the FE size and on the thickness, according to Lehmann and Peschmann [24].

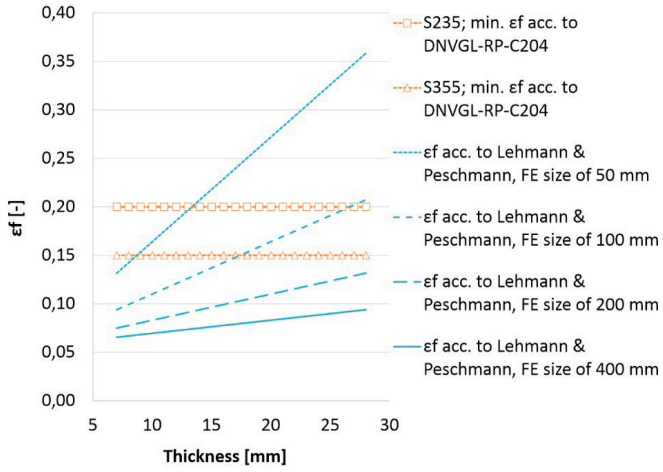

Fig. 8. Failure strain εf according to the DNVGL-RP-C204 [38] and Lehmann and Peschmann [24].

The strain rate dependency for steel was defined using the Cowper-Symonds model [46] according to Eq. (3). The material coefficients are C=500 s^{-1} (p=4) for steel S235 and C=3200 s^{-1} (p=5) for steel S355 [45-47].

$$\beta = 1 + \left(\frac{\dot{\varepsilon}}{C}\right)^{\frac{1}{p}} \tag{3}$$

where:
$\dot{\varepsilon}$ – strain rate,
C, p – material constraints.

THE FE MESH CONVERGENCE

The analysis of the finite element mesh convergence was performed for FE sizes 50, 100, 200 and 400 mm. The criterion used was the internal energy, which was analysed for different FE element sizes. It was found that the use of the 100 mm elements was the right choice as this size represented a compromise between the accuracy of the results obtained and the computational cost. A similar discretisation was used in [22] and [48]. The difference in the value of the maximum internal energy was 2% for the 50 mm and 100 mm element sizes. The difference between 100 mm and 200 mm was 8% and, for 100 mm and 400 mm, it was 21%.

RESULTS AND DISCUSSION

The results presented below refer to the computer simulations for three initial velocities of the ship: 2, 3 and 4 m/s. These speed increments increased the kinetic energy of the ship's collision with the support column of the offshore wind turbine and the energy was converted into internal energy, corresponding to the work applied to deform the ship's structure. The greater the initial collision energy, the greater the expected damage to the ship's structure. The simulations were also performed for two materials: normal-strength steel S235 and high-strength steel S355. The effect of the damage criteria was analysed for both material curves. The strongly non-linear nature of the simulations affects the calculated resultant damage to the ship. The influence of the two selected material failure criteria and the influence of the two representations of the material model curve were investigated. Typical physical quantities, such as the crushing force and the internal energy, were used for comparison purposes. The hull damage resulting from the collision was analysed using the length of the ship's hull rupture, L_r, and the area of the hull opening, A_o. The aforementioned simulation cases were solved and they delivered the following results, which will be discussed as groups, devoted to separate aspects.

THE INFLUENCE OF THE MATERIAL STRESS-STRAIN CURVE REPRESENTATION

The first group of results show the influence of the stress-strain curve representation on the collision results. The first curve used was a simplified representation, in accordance with the DNV GL 2013 design rules [40]. This approach was used for many years but has been changed, quite recently. The second representation of the material relation presents the most recent definition of the curve, according to the DNV GL 2019 design rules [31]. The curve was discretised with a strain step of 0.01. Such a definition aimed to ensure more accurate representation of the curve, especially in its non-linear range corresponding to plastic deformations. A strong influence of the material model representation by the stress-strain curve, according to DNV GL 2013 [40] and DNV GL 2019 [31], on the ship's damage was found (see Fig. 9). The

analysis was performed for the material failure criterion according to Lehmann and Peschmann [24]. The simplified curve representation, according to DNV GL 2013 [40], gave an overestimation of ship's damage, as measured by the area of the hull opening, Ao. Moreover, the results showed that this influence varied depending on the analysed initial ship velocities and steel grades. This can be explained by very high non-linearity of collision simulations. The highest divergence between the crushing forces and the resultant hull damage was found for the velocity of 4 m/s for both steel grades (S235 and S355). It is also noticeable that, even for comparable crushing forces, the resultant hull damage differed significantly (see the crushing force and the hull damage for steel S355 and for v = 4 m/s in Fig. 9).

and the Lehmann and Peschmann [24]. The influence of the failure criterion on the hull damage and internal energy, until the decoupling of the ship and the OWT, are shown in Fig. 10. In this analysis, the material stress-strain curve was modelled according to DNV GL 2019 [31]. The literature review presented in section 1 revealed significant differences in the values of failure strain used by various authors. The common value of the rupture strain, $\varepsilon_f = 0.2$ for S235 and $\varepsilon_f = 0.15$ for S355, was validated against the experimental results [38]. Other studies used different values, including the criterion in [24], which was recently implemented in [31]. The relationship includes the influence of the FE size and the shell thickness, to calculate the corrected value of the rupture strain. The comparison performed on these two

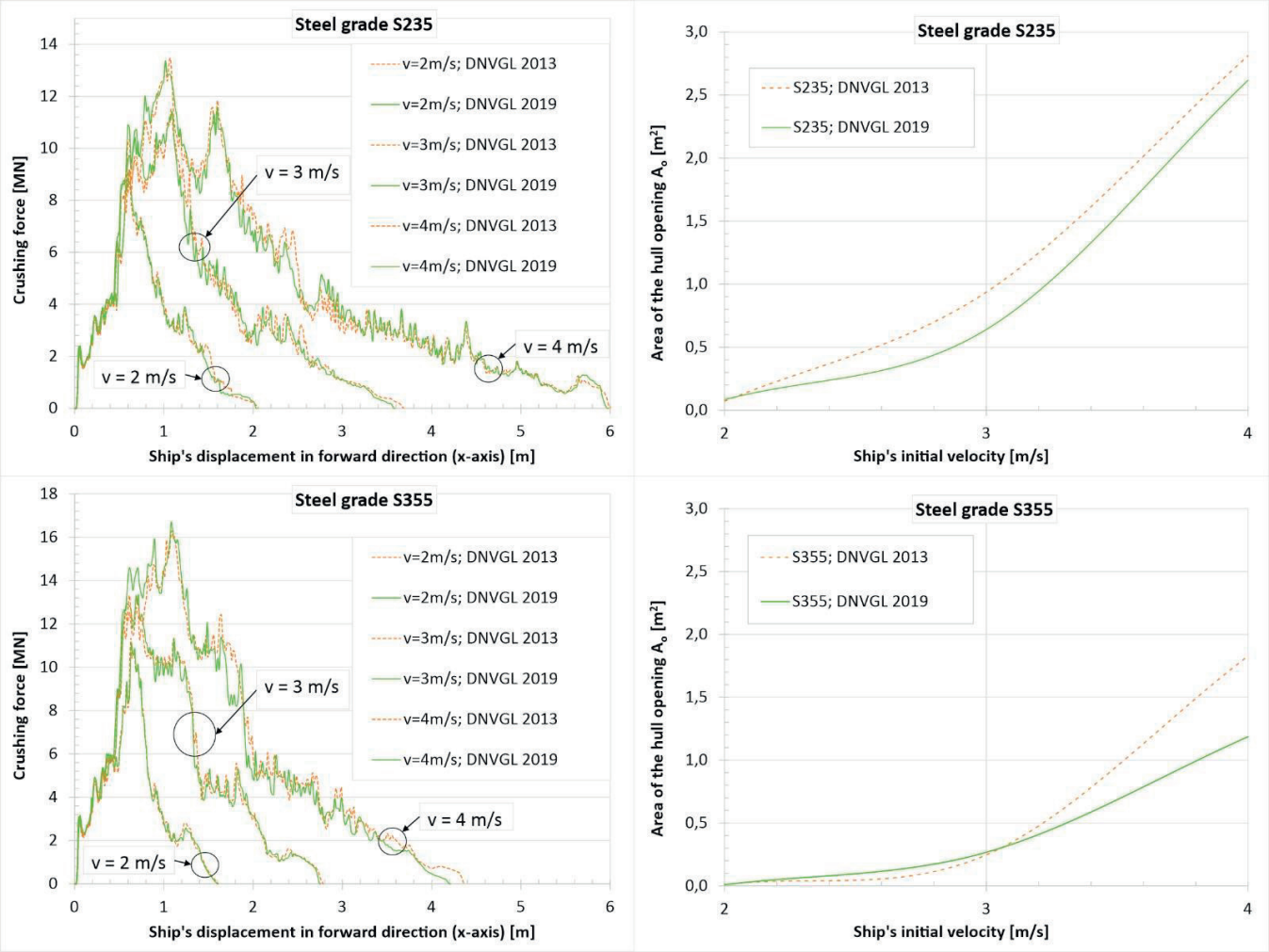

Fig. 9. The influence of the material stress-strain curve representation on the crushing force (left) and on the ship's hull damage (right).

THE INFLUENCE OF THE SELECTED STRAIN-BASED FAILURE CRITERIA

The following section presents the results of the collision simulations for the two material failure criteria, ε_f, as described in section 3.2, namely DNVGL-RP-C204 [38]

failure criteria showed a strong influence on the results. In the example of steel grade S235 and for the ship's initial velocity of 4 m/s, the calculated relative maximum crushing force differed by as much as 20%. As a result, the internal energies for both failure criteria were very different. Consequently, for different assumptions of the damage criterion, the resulting hull damage varied considerably. In the example with S235 steel grade and an initial ship's velocity of 4 m/s, the calculated hull shell rupture, L_r was equal to 1.38 m and 9.32 m for the

minimum required ε_f, according to the DNVGL-RP-C204 [38] and Lehmann and Peschmann [24] failure criterion, respectively. The areas of hull opening, A_o, were 0.26 m^2 and 2.62 m^2, respectively. Thus, for S235 steel, the case using the $\varepsilon_f = 0.2$ criterion leads to a major underestimation of the hull damage. The influence was similar, but smaller, for S355 steel. For the initial ship's velocity of 4 m/s, the calculated hull shell rupture, L_r, was equal to 1.90 m and 4.56 m for the failure criteria [38] and [24], respectively. The area of the hull opening, A_o, was 0.43 m^2 and 1.19 m^2, respectively. As described above, the use of criterion DNV GL-RP-C204 [38] resulted in a significant underestimation of the ship's hull damage. Fig. 10 shows the internal energy plots for the analysed damage criteria and for the initial ship's velocities. The effect of the failure criteria analysed is more pronounced for the normal-strength steel S235 and, as expected, amplified with increasing impact energy. For all the analysed cases, the maximum internal energy was found in the Lehmann and Peschmann failure criterion [24]. However, for the initial velocities of the ship at 3 m/s and 4 m/s, in the initial phase of impact for criterion DNV GL-RP-C204 [38], the value of internal energy was higher, which corresponded to larger plastic deformation of the ship's structure. It is worth noting that the slopes of the curves were slightly different and intersected each other, leading to significantly different damage resulting from the conversion of the ship's kinetic energy into plastic deformation.

For all analysed cases, the accelerations of a ship's centre of gravity (COG) for the S355 steel were higher compared to S235. For the Lehmann and Peschmann failure criterion [24] the average difference was 25%. For the criterion DNV GL-RP-C204 [38], it was 12%, on average. The resultant hull damage for the analysed simulation cases and initial ship speed of 4 m/s, are shown in Fig. 11. The hull damage presented perfectly illustrates the relations resulting from the influence of the analysed failure criteria and the method of the material curve representation.

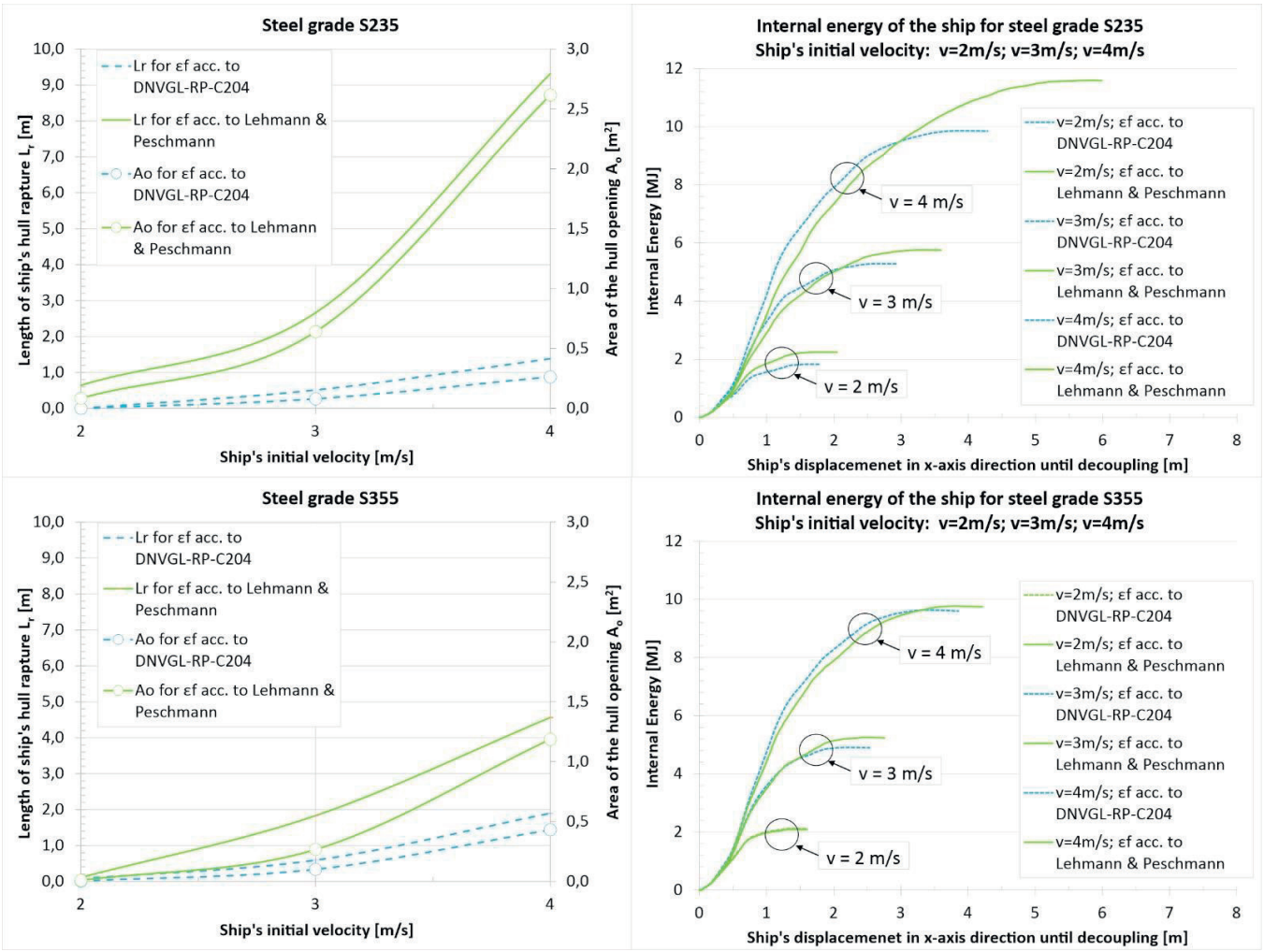

Fig. 10. The influence of the material failure criterion, εf, on the hull damage (left) and on the internal energy (right).

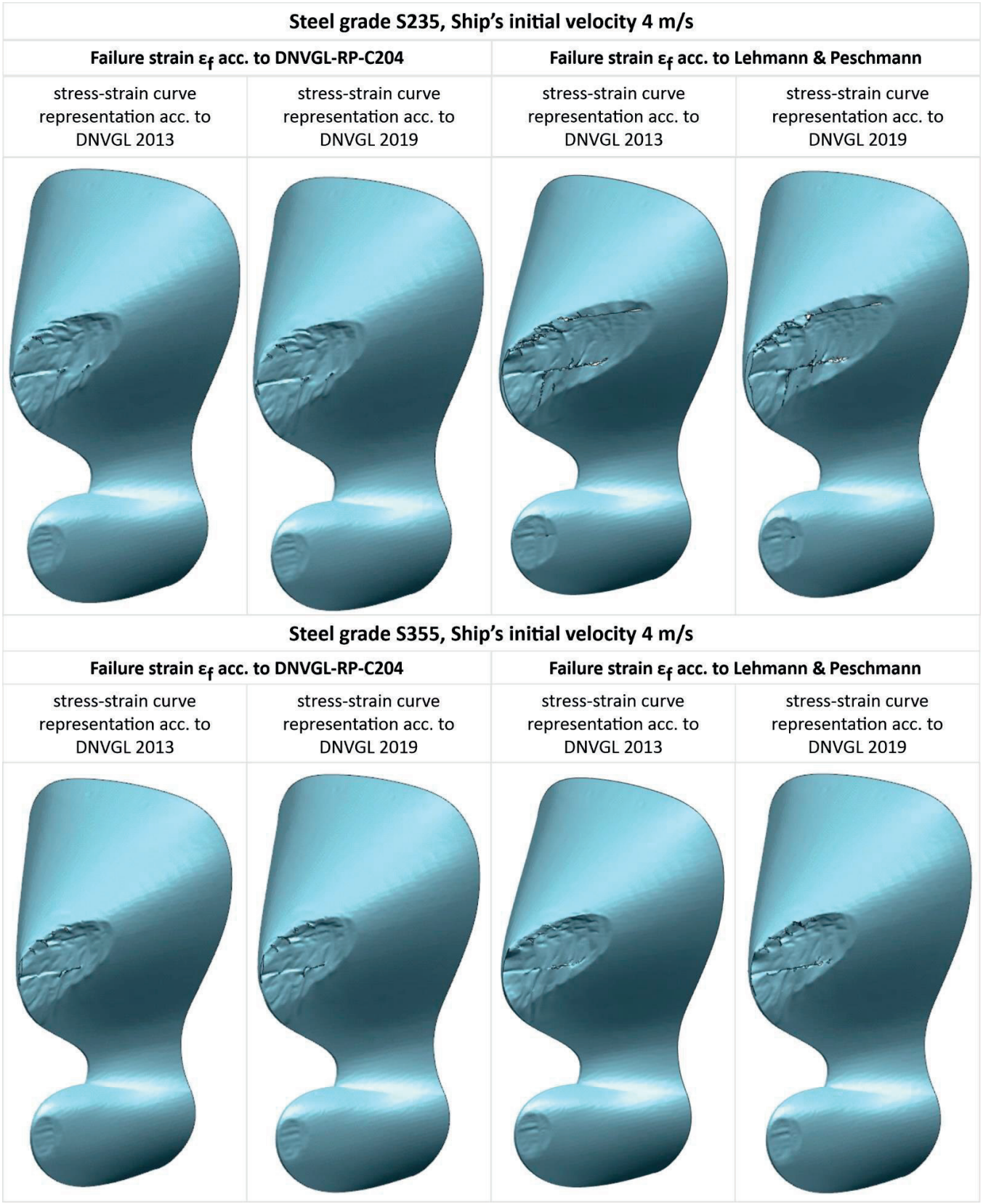

Fig. 11. The resultant hull damage for the analysed cases and the ship's initial velocity of 4 m/s.

CONCLUSIONS

The analysis of collision resistance of ships and offshore structures requires performing highly non-linear FE simulations. One of the main computational assumptions is the material model, including the failure criteria. So far, there are no straightforward design recommendations defining the proper approach to this. The literature review showed various modelling assumptions used by the authors. Thus, this article investigated the influence of the selected strain-based failure criteria and material modelling representations on the simulation results of ship collisions with OWT monopiles. The following conclusions were formulated:

1) The influence of the modelling of the material curve has a significant influence on the results. In highly non-linear simulations, like those of collisions, the simplification of the material stress-strain relation by straight lines plotted by characteristic points is too rough and can lead to inaccurate or erroneous results. The non-linear range of the material stress-strain relation needs to be represented by an adequate number of points. There is no specific guideline on how dense the representation should be. It was verified that, using the material modelling recommendation according to DNV GL 2013 [40] (which represents the material characteristics by 6 points (5 straight curves)), had a significant influence on the results. For steel S235, the values of the crushing force were up to 12% different from the results obtained from the simulations based on the accurately mapped material curve according to DNV GL 2019 [31]. Although the maximum value of the crushing force was determined correctly by the simplified material curve, the energy dissipation was changed. As a consequence, the resulting hull damage was significantly different for the analysed material modelling representations (DNV GL 2013 [40] and DNV GL 2019 [31]). In an example with an initial ship velocity of 4 m/s and steel S235, the hull plating opening, A_o, was 7% higher for the simplified curve representation [40]. For steel grade S355, the corresponding relative difference was as much as 54%. Using the simplified material curve leads to an overestimation of the resultant hull damage (on the 'safe side' from an engineering point of view). However, it does not necessarily have to be beneficial, from a design point of view, and can lead to oversized structural components, which has a negative influence on both the cost and weight.
2) The impact of the material's failure criterion is crucial. The performed comparison of the collision results obtained with the use of the two selected failure criteria showed the importance of this computational assumption. In the example with steel grade S235 and with an initial ship velocity of 4 m/s, the calculated relative maximum crushing force differed by as much as 20%. As a result, the internal energies were very different for each of the failure criteria. The resultant hull damage varied considerably for the failure criteria according to DNV GL-RP-C204 [38]. The first one lead to significantly lower hull damage. In the example with steel S235 and with the initial ship's velocity of 4 m/s, the calculated hull damage was underestimated by up to 6 times for the length of the hull rupture and 9 times for the area of the hull opening. The observation was similar for steel grade S355, however, the impact on the results was relatively smaller. For steel grade S355 and the failure criterion, ε_f, as the minimum required value, according to DNV GL-RP-C204 [38], there was an underestimation of the length of the hull rupture by 1.4 times and of the hull opening by 1.8 times. Thus, it can be concluded that performing collision simulations with an assumption of failure criteria equal to the minimum values defined by DNV GL-RP-C204 [38] can significantly underestimate the hull damage. The applied failure criterion should account for the effect of the FE element size and the material thickness, as in Lehmann and Peschmann [24]. The analysis of a collision may also consider using different failure criteria and comparing the results to those with a reasonable approach, resulting from risk assessment.
3) Although it was not the purpose of this paper, a significant influence of steel grade on the ship's hull failure was found. The relative reduction of the length of the S355 hull plating rupture was -31% and -51% for the ship's initial velocities of 3 m/s and 4m/s, respectively. Moreover, the relative reduction of the hull opening area was -58% and -55%. The influence of the steel grade selection on the hull damage is highly visible and will be investigated by the authors in detail in future research.

ACKNOWLEDGEMENTS

The research was supported by the Academic Computer Centre in Gdansk (CI TASK). All support is highly appreciated by the authors.

REFERENCES

1. L. Ramirez, D. Fraile, and G. Brindley, "Offshore wind in Europe: Key trends and statistics 2019," 2019.

2. L. Ramirez, D. Fraile, and G. Brindley, "Offshore wind in Europe: Key trends and statistics 2020," 2021.

3. EMSA, "Marine Casualties and Incidents PRELIMINARY ANNUAL OVERVIEW OF MARINE CASUALTIES AND INCIDENTS 2014-2020," no. April, 2021.

4. L. Junlai, X. Yonghe, W. Weiguo, and Z. Chi, "Analysis of the Dynamic Response of Offshore Floating Wind Power Platforms in Waves," Polish Marit. Res., vol. 27, no. 4, pp. 17–25, 2020. doi: 10.2478/pomr-2020-0062

5. A. Karczewski and Ł. Piątek, "The influence of the cuboid float's parameters on the stability of a floating building," Polish Marit. Res., vol. 27, no. 107, pp. 16–21, 2020. doi: 10.2478/pomr-2020-0042

6. K. Niklas and A. Karczewski, "Determination of seakeeping performance for a case study vessel by the strip theory method," Polish Marit. Res., vol. 27, no. 108, pp. 4–16, 2020. doi: 10.2478/pomr-2020-0061

7. F. Wang and N. Chen, "Dynamic response analysis of drill pipe considering horizontal movement of platform during installation of subsea production tree," Polish Marit. Res., vol. 27, no. 3, pp. 22–30, 2020. doi: 10.2478/pomr-2020-0043

8. J.T. Wu, J.H. Chen, C.Y. Hsin, and F.C. Chiu, "Dynamics of the FKT System with Different Mooring Lines," Polish Marit. Res., vol. 26, no. 1, pp. 20–29, 2019. doi: 10.2478/pomr-2019-0003

9. E. Mieloszyk, M. Abramski, and A. Milewska, "CFGFRPT Piles with a Circular Cross-Section and their Application in Offshore Structures," Polish Marit. Res., vol. 26, no. 3, pp. 128–137, 2019. doi: 10.2478/pomr-2019-0053

10. W. Litwin, W. Leśniewski, D. Piątek, and K. Niklas, "Experimental Research on the Energy Efficiency of a Parallel Hybrid Drive for an Inland Ship," Energies, vol. 12, no. 9, p. 1675, 2019.

11. V.S. Blintsov, K.S. Trunin, and W. Tarełko, "Determination of Additional Tension in Towed Streamer Cable Triggered by Collision with Underwater Moving Object," Polish Marit. Res., vol. 27, no. 2, pp. 58–68, 2020. doi: 10.2478/pomr-2020-0027

12. K. Niklas and H. Pruszko, "Full scale CFD seakeeping simulations for case study ship redesigned from V-shaped bulbous bow to X-bow hull form," Appl. Ocean Res., vol. 89, pp. 188–201, Aug. 2019.

13. F. Biehl, "Collision Safety Analysis of Offshore Wind Turbines," 4th LSDYNA Eur. Conf., pp. 27–34, 2005.

14. K. Niklas, "Strength analysis of a large-size supporting structure for an offshore wind turbine," Polish Marit. Res., vol. 24, pp. 156–165, 2017. doi: 10.1515/pomr-2017-0034

15. P. Dymarski, "Design of Jack-Up Platform for 6 MW Wind Turbine: Parametric Analysis Based Dimensioning of Platform Legs," Polish Marit. Res., vol. 26, no. 2, pp. 183–197, 2019. doi: 10.2478/pomr-2019-0038

16. B. Rozmarynowski, "Spectral Dynamic Analysis of A Stationary Jack-Up Platform," Polish Marit. Res., vol. 26, no. 1, 2019. doi: 10.2478/pomr-2019-0005

17. WindEurope, "Offshore wind in Europe - Key trends and statistics 2020," WindEurope, vol. 3, no. 2, pp. 14–17, 2021.

18. N. Ren and J. Ou, "Dynamic numerical simulation for ship-OWT collision," Proc. 2009 8th Int. Conf. Reliab. Maintainab. Safety, ICRMS 2009, no. July, pp. 1003–1007, 2009.

19. E. Homayoun, H. Ghassemi, and H. Ghafari, "Power Performance of the Combined Monopile Wind Turbine and Floating Buoy with Heave-Type Wave Energy Converter," Polish Marit. Res., vol. 26, no. 3, pp. 107–114, 2019. doi: 10.2478/pomr-2019-0051

20. J.R.A.Tomporowski, A.Al-Zubiedy, J.Flizikowski, W.Kruszelnicka, P.Bałdowska-Witos, "Analysis of the Project of innovative floating turbine," Polish Marit. Res., vol. 26, no. 4, pp. 121–183, 2020. doi: 10.2478/pomr-2019-0074

21. A. Bela, L. Buldgen, P. Rigo, and H. Le Sourne, "Numerical crashworthiness analysis of an offshore wind turbine monopile impacted by a ship," Anal. Des. Mar. Struct. - Proc. 5th Int. Conf. Mar. Struct. MARSTRUCT 2015, no. 2013, pp. 661–669, 2015.

22. A. Bela, H. Le Sourne, L. Buldgen, and P. Rigo, "Ship collision analysis on offshore wind turbine monopile foundations," Mar. Struct., vol. 51, pp. 220–241, 2017.

23. H. Jia, S. Qin, R. Wang, Y. Xue, D. Fu, and A. Wang, "Ship collision impact on the structural load of an offshore wind turbine," Glob. Energy Interconnect., vol. 3, no. 1, pp. 43–50, 2020.

24. E. Lehmann and J. Peschmann, "Energy absorption by the steel structure of ships in the event of collisions," Mar. Struct., vol. 15, no. 4–5, pp. 429–441, 2002.

25. K. Niklas and J. Kozak, "Experimental investigation of Steel-Concrete-Polymer composite barrier for the ship internal tank construction," Ocean Eng., vol. 111, pp. 449–460, 2016.

26. Ringsberg, J., Amdahl, J., Chen, B., Cho, S.-R., Ehlers, S., Hu, Z., Kubiczek, J., Kõrgesaar, M., Liu, B., Marinatos, J., Niklas, K., Parunov, J., Quinton, B., Rudan, S., Samuelides, M., Soares, C., Tabri, K., Villavicencio, R., Yamada, Y., Yu, Z., & Zhang, S., "MARSTRUCT benchmark study on nonlinear FE simulation of an experiment of an indenter impact with a ship side-shell structure," Mar. Struct., vol. 59, pp. 142–157, 2018.

27. A. AbuBakar and R.S. Dow, "The impact analysis characteristics of a ship's bow during collisions," Eng. Fail. Anal., vol. 100, no. August 2018, pp. 492–511, 2019.

28. K. Niklas, "Numerical calculations of behaviour of ship double-bottom structure during grounding," Polish Marit. Res., vol. 15, no. SUPPL. 1, 2008.

29. M.A.G. Calle and M. Alves, "A review-analysis on material failure modelling in ship collision," Ocean Eng., vol. 106, pp. 20–38, 2015.

30. O. Kitamura, "FEM approach to the simulation of collision and grounding damage," Mar. Struct., vol. 15, no. 4–5, pp. 403–428, 2002.

31. DNVGL, "DNV-RP-C208: Determination of Structural Capacity by Non-linear FE analysis Methods," 2019.

32. J.L. Martinez, J.C.R. Cyrino, and M.A. Vaz, "FPSO collision local damage and ultimate longitudinal bending strength analyses," Lat. Am. J. Solids Struct., vol. 17, no. 2, pp. 1–19, 2020.

33. G. Wang, K. Arita, and D. Liu, "Behavior of a double hull in a variety of stranding or collision scenarios," Mar. Struct., vol. 13, no. 3, pp. 147–187, 2000.

34. S. Yagi, H. Kumamoto, O. Muragishi, Y. Takaoka, and T. Shimoda, "A study on collision buffer characteristic of sharp entrance angle bow structure," Mar. Struct., vol. 22, no. 1, pp. 12–23, 2009.

35. S. Ehlers, "The influence of the material relation on the accuracy of collision simulations," Mar. Struct., vol. 23, no. 4, pp. 462–474, 2010.

36. S. Ehlers, J. Broekhuijsen, H.S. Alsos, F. Biehl, and K. Tabri, "Simulating the collision response of ship side structures: A failure criteria benchmark study," Int. Shipbuild. Prog., vol. 55, no. 1–2, pp. 127–144, 2008.

37. Standards Norway, "NORSOK Standard - Design of steel structure N-004, Rev.3," 2013.

38. DNVGL, "DNVGL-RP-C204 - Design against Accidental Loads," 2017.

39. M. Scharrer, L. Zhang, and E.D. Egge, "Final report MTK0614, Collision calculations in naval design systems, Report Nr. ESS 2002.183," Hamburg, 2002.

40. DNVGL, "DNV-RP-C208: Determination of Structural Capacity by Non-linear FE analysis Methods," 2013.

41. S. Zhang, "The mechanics of ship collisions," Technical University of Danemark, 1999.

42. Verband Deutscher Ingenieure, "Systematic calculation of high duty bolted joints joints with one cylindrical bolt," Berlin, 2003.

43. O. Ozgur, "Numerical Assessment of FPSO Platform Behaviour in Ship Collision," Trans. Marit. Sci., vol. 9, no. 2, 2020.

44. T. S. Bøe, "Analysis and Design of Stiffened Columns in Offshore Floating Platforms Subjected to Supply Vessel Impacts," Norwegian University of Science and Technology, 2018.

45. M.P. Mujeeb-Ahmed, S.T. Ince, and J.K. Paik, "Computational models for the structural crashworthiness analysis of a fixed-type offshore platform in collisions with an offshore supply vessel," Thin-Walled Struct., vol. 154, no. June, p. 106868, 2020.

46. Livermore Software Technology, "LS-DYNA - KEYWORD USER'S MANUAL, VOLUME II Material Models," 2020.

47. Y.G. Ko, S.J. Kim, J.M. Sohn, and J.K. Paik, "A practical method to determine the dynamic fracture strain for the nonlinear finite element analysis of structural crashworthiness in ship–ship collisions," Ships Offshore Struct., vol. 13, no. 4, 2018.

48. J. Travanca and H. Hao, "Energy dissipation in high-energy ship-offshore jacket platform collisions," Mar. Struct., vol. 40, pp. 1–37, 2015.

CONTACT WITH THE AUTHORS

Karol Niklas
e-mail: karol.niklas@pg.edu.pl

Gdansk University of Technology,
Faculty of Mechanical Engineering and Ship Technology,
Narutowicza 11/12, 80-233 Gdansk,
Poland

Alicja Bera
e-mail: alicja.bera@pg.edu.pl

Gdansk University of Technology,
Faculty of Mechanical Engineering and Ship Technology,
Narutowicza 11/12, 80-233 Gdansk,
Poland